What Drives Turbulence in Spontaneous Reconnection?

Grzegorz Kowal

University Cruzeiro do Sul, São Paulo, Brazil

Collaborators: D. A. Falceta-Gonçalves (EACH-USP, Brazil)
A. Lazarian (UW-Madison, USA)
E. T. Vishniac (JHU, USA)

and many others from related projects

Magnetic Fields in the Universe VI, Natal, Brazil, Oct. 16-20, 2017

Outline

- First models of magnetic reconnection – addressing the problem of inefficient reconnection rate.
- The role of turbulence on reconnection – the LV99 model and its numerical testing.
- Reconnection-driven turbulence and its statistics.
- Processes responsible for turbulence driving in stochastic reconnection.

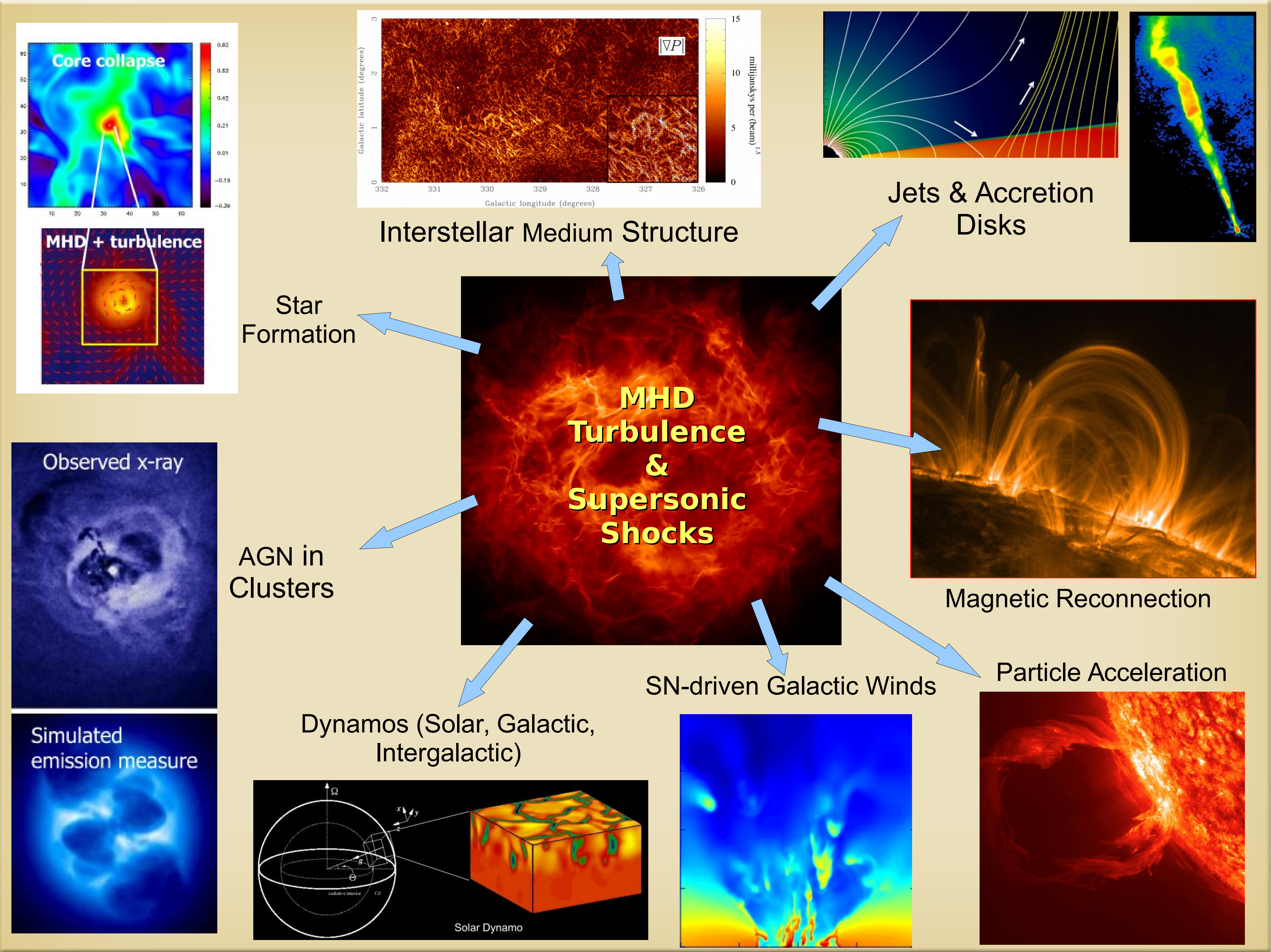
Core collapse
MHD + turbulence
Star Formation
|∇P|
Galactic latitude (degrees)
Galactic longitude (degrees)
millijanskys per (beam)
Interstellar Medium Structure
Jets & Accretion Disks
MHD Turbulence & Supersonic Shocks
Magnetic Reconnection
Observed x-ray
Simulated emission measure
AGN in Clusters
Particle Acceleration
SN-driven Galactic Winds
Dynamos (Solar, Galactic, Intergalactic)
Solar Dynamo

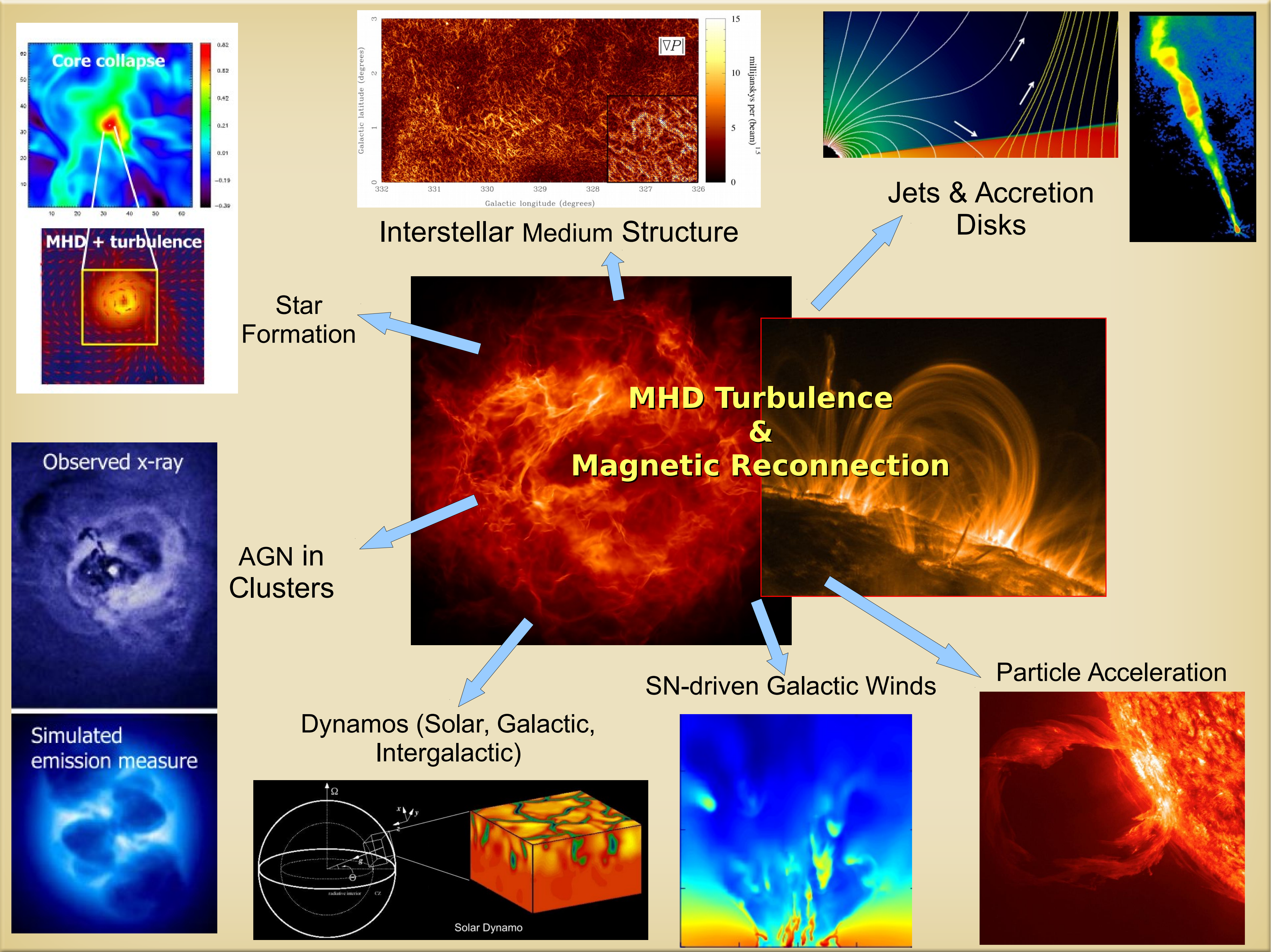
Core collapse
MHD + turbulence
Galactic latitude (degrees)
Galactic longitude (degrees)
|∇P|
millijanskys per (beam)
Interstellar Medium Structure
Jets & Accretion Disks
Star Formation
MHD Turbulence
&
Magnetic Reconnection
Observed x-ray
Simulated emission measure
AGN in Clusters
Dynamos (Solar, Galactic, Intergalactic)
Solar Dynamo
SN-driven Galactic Winds
Particle Acceleration

Flux-Freezing Breakdown in MHD Turbulence

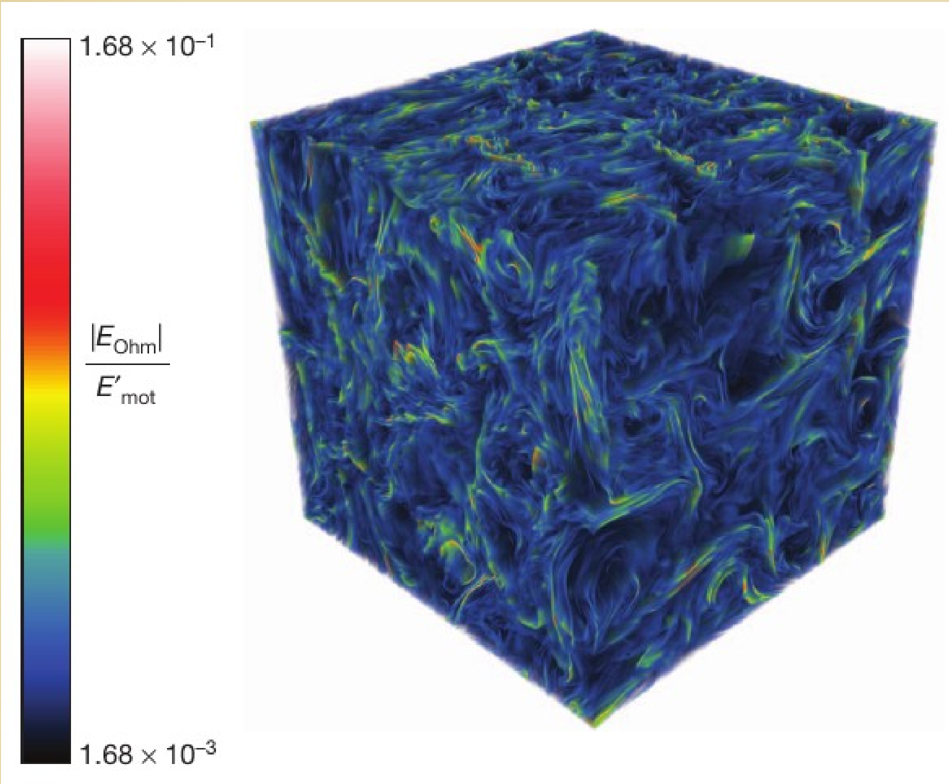

Eyink et al. (2013)

Ohmic electric field E_{Ohm} = J/σ normalized by the r.m.s. value, E'_{mot}, of the motional field, E_{mot} = - v×B/c, for one 1,024^3-point time slice of the archived data. The colour scale covers a range from 0.1 to 10 times the r.m.s. value, 1.68×10^{-2}, of the normalized Ohmic field. The Ohmic electric field is negligible compared with the motional field, except in the most intense current sheets.

Kowal et al. (2017, in prep.)

The magnetic shear angle rate θ in a compressible MHD model with M_s = 1.0 and M_A = 1.0.

$$\theta = \cos^{-1} \frac{\vec{B}_i \cdot \vec{B}_j}{|\vec{B}_i||\vec{B}_j|}$$

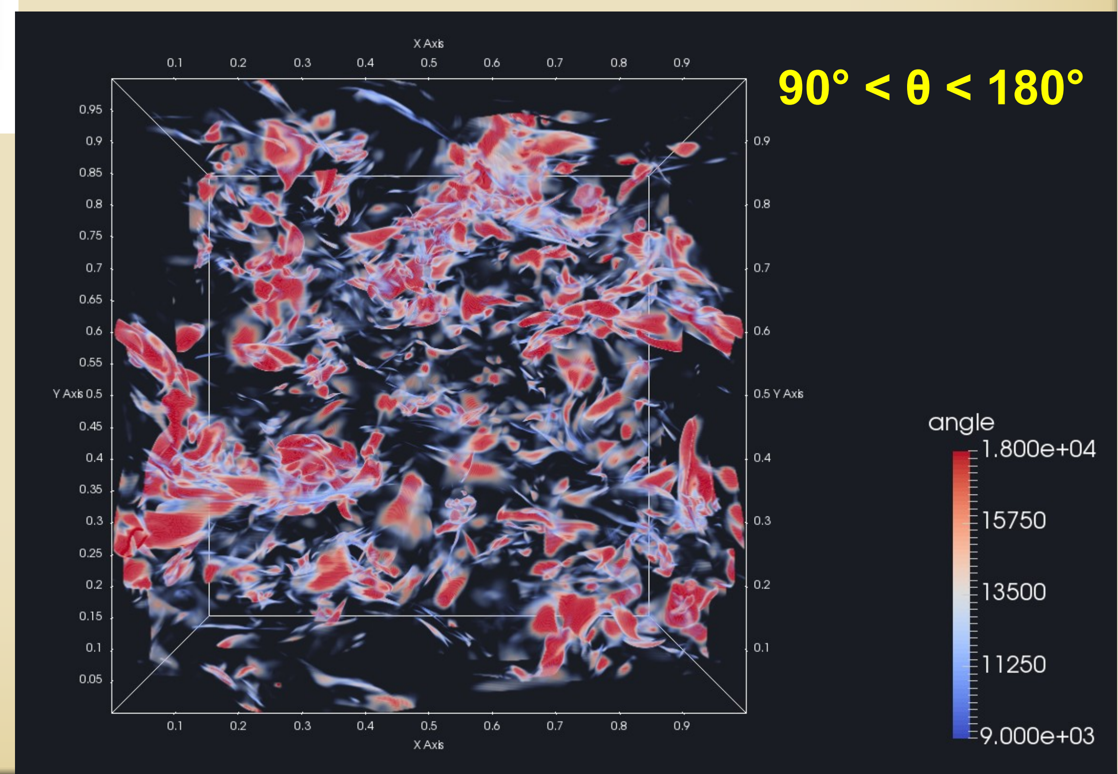

Sweet-Parker model (1957)

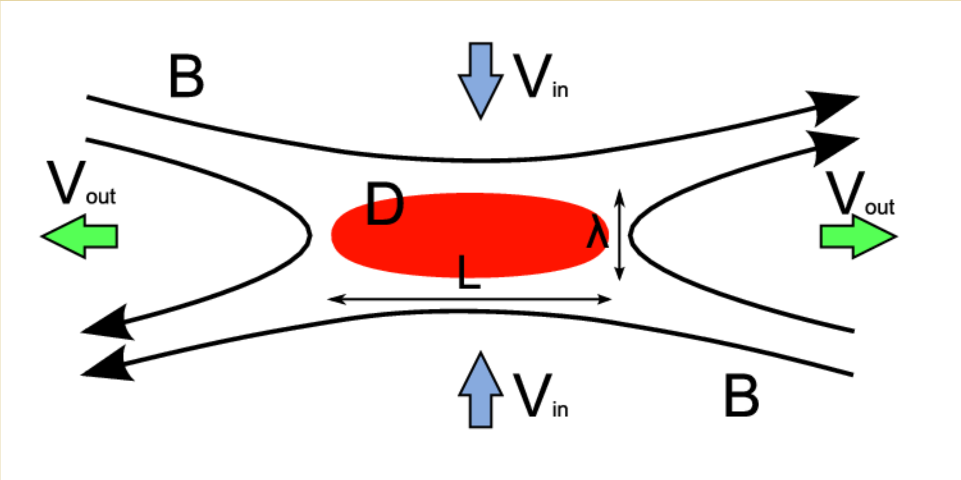

$$V_{inflow} = \eta/\lambda$$

Ohmic diffusion

$$V_{inflow} L = V_{outflow} \lambda$$

Mass conservation

$$V_{outflow} = V_A$$

Free outflow

Reconnection Rate:

$$V_{inflow} = V_A \left(\frac{\lambda}{L} \right) = V_A \left(\frac{L V_A}{\eta} \right)^{-1/2} = V_A S_L^{-1/2}$$

Lundquist Number

PROBLEM: S_L very large for astrophysical objects!

Solar Corona $S_L \sim 10^{12}$-10^{14}, ISM $S_L \sim 10^{15}$-10^{20}

How to make reconnection faster?

Alternative Models

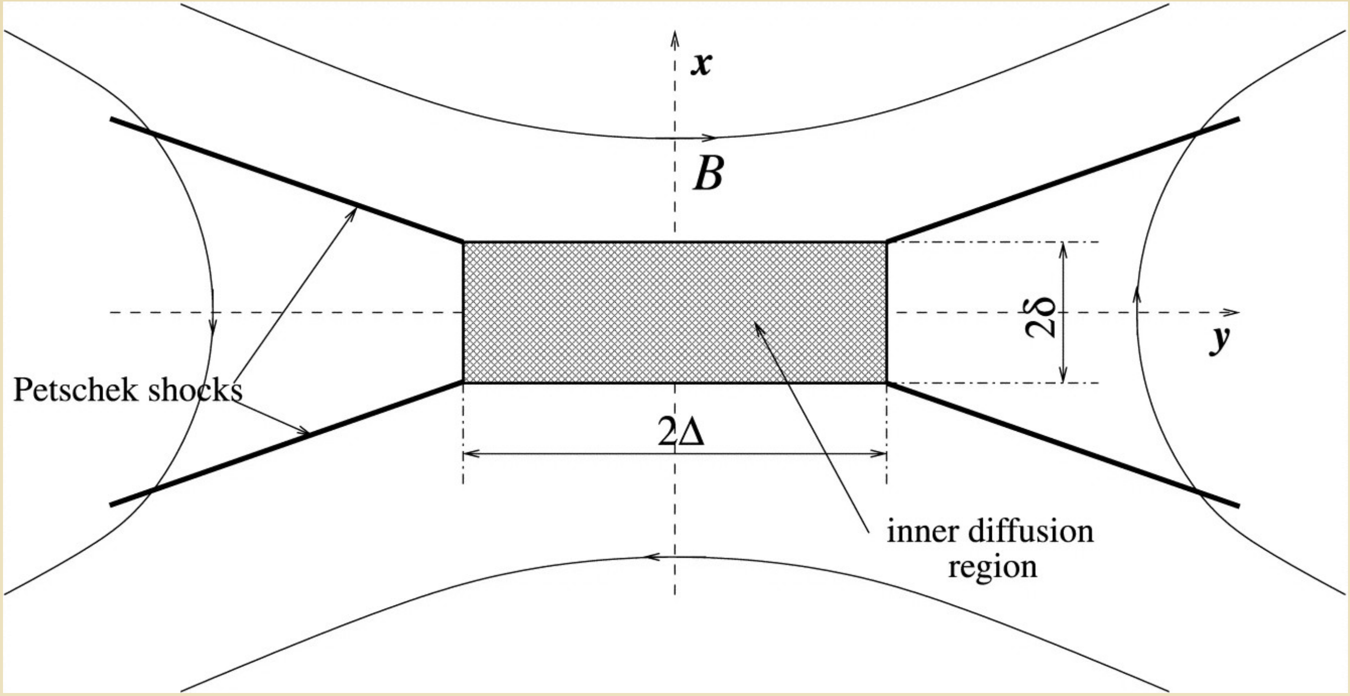

Reconnection Rate:

Petschek (1964)

$$V_{inflow} = V_A \left(\frac{\pi}{8 \ln S_L} \right)$$

Simulations with uniform resistivity show that Petschek model is **unstable** and shortly becomes Sweet-Parker type. To stabilize it we need a localized anomalously large resistivity. Because the use of an anomalous resistivity is only appropriate when the particle mean free path is large compared to the reconnection layer, it is likely that other collisionless effects become important before Petschek reconnection can be realized.

Biskamp (1996, 2000)

Introducing a Weak Stochastic Component

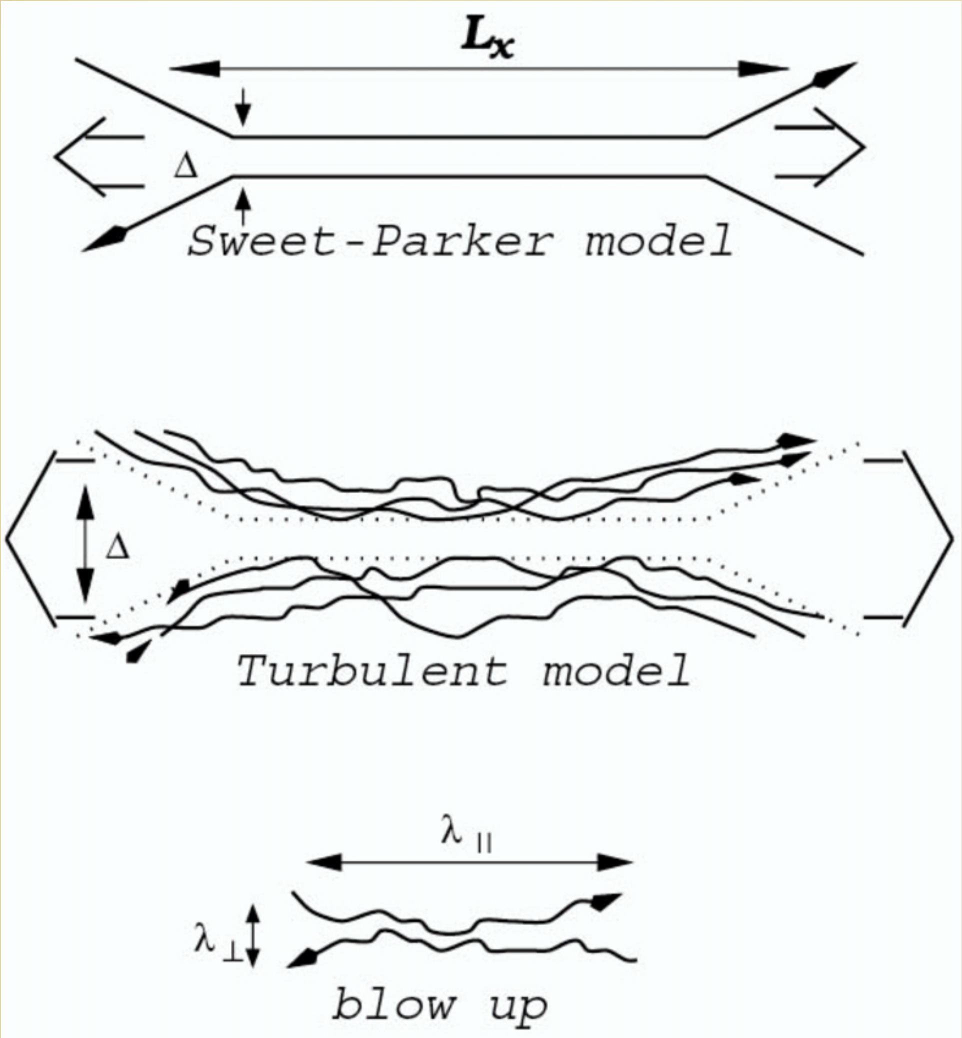

B dissipates on a small scale $\lambda_{\parallel}$ determined by turbulence statistics.

Lazarian & Vishniac (1999)

Reconnection of 3D turbulent magnetic field involves simultaneous reconnection events

Key element: $L/\lambda_{\parallel}$ events!

Turbulent reconnection:

- Thick current sheet determined by field wandering.
- Reconnection is fast with Ohmic resistivity only.

$$V_{inflow} = \frac{L}{\lambda_{\parallel}} V_{rec,\,local}$$

$$V_{rec} < V_A \, min \left[\left(\frac{L}{\lambda_{\parallel}} \right)^{1/2}, \left(\frac{\lambda_{\parallel}}{L} \right)^{1/2} \right] \left(\frac{V_T}{V_A} \right)^2$$

Sweet-Parker vs Turbulent Reconnection

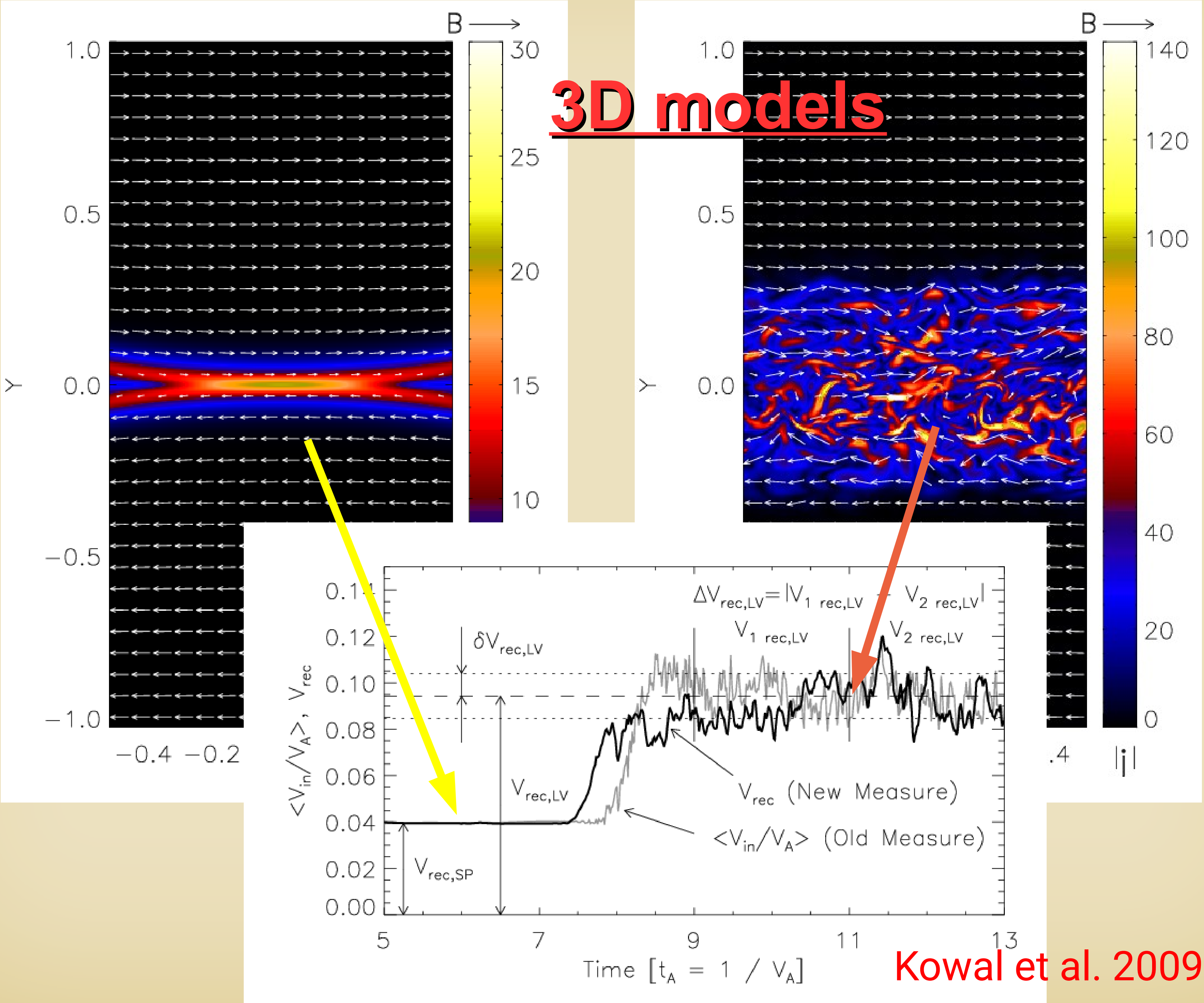

Kowal et al. 2009, 2012

Dependencies on Power and Injection Scale

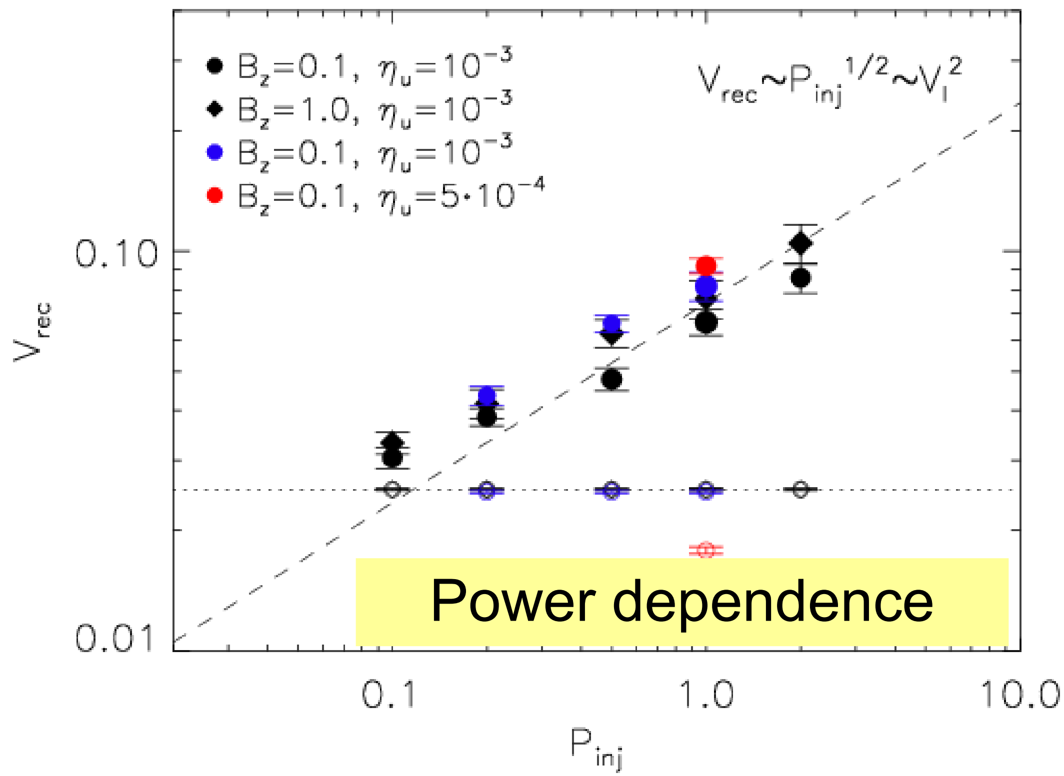

Upper limit imposed by the large-scale field line diffusion

$$V_{rec} < V_A \min\left(\frac{l_{inj}}{L}\right)^{1/2}\left(\frac{v_{inj}}{V_A}\right)^2$$

Lazarian & Vishniac (1999)

Kowal et al. (2009, 2012)

- Fourier space driving of the velocity
- Real space random driving of the velocity
- Real space driving of the magnetic field

Power-velocity conversion

$$P = \epsilon_l = \frac{v_l^2}{\tau_l} = \frac{v_L^2\,(l/L)^{-2/3}}{(L/v_L)\,(l/L)^{-2/3}}\,\frac{(v_L/V_A)^{2/3}}{(v_L/V_A)^{-1/3}} = \frac{v_L^4}{V_A L}$$

from GS95

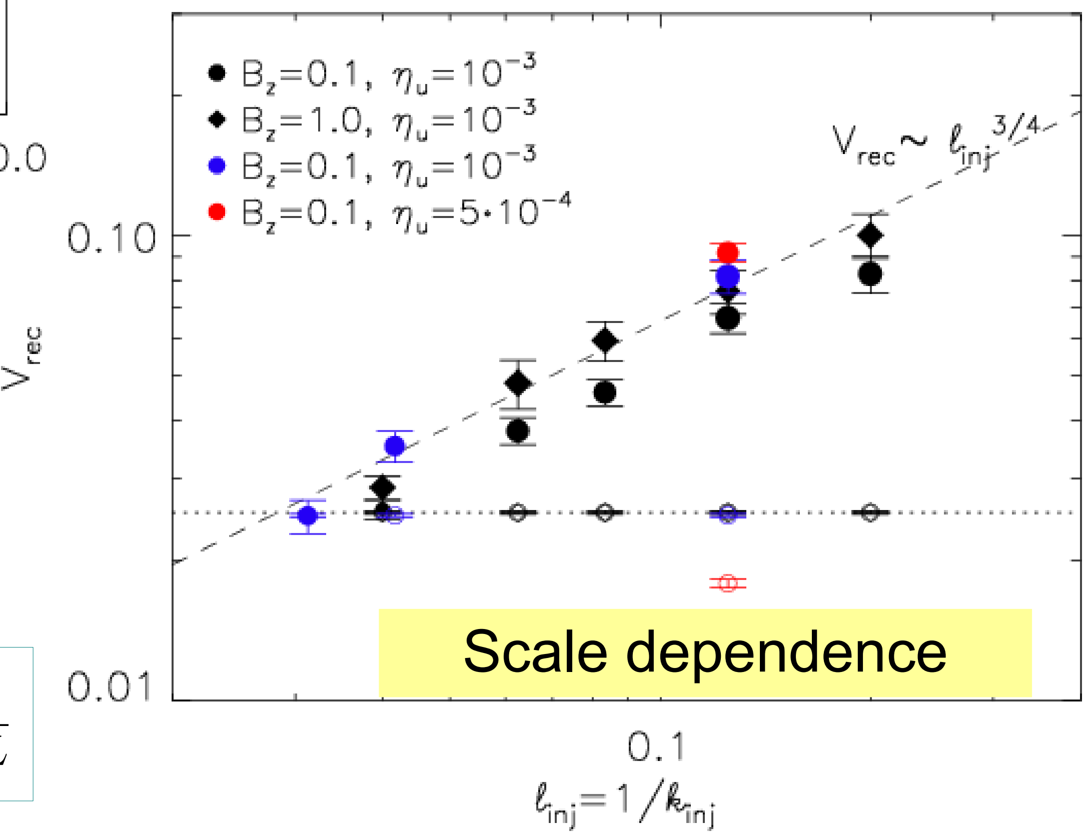

Dependence on Resistivity

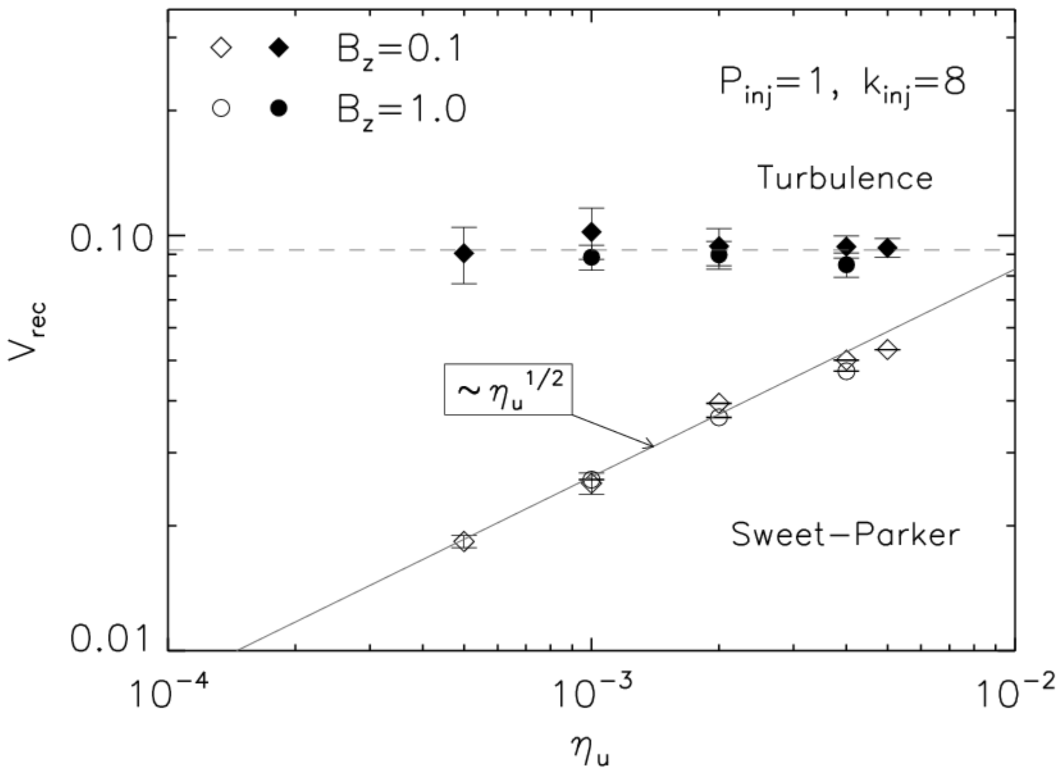

The reconnection rate does not depend on the Ohmic resistivity, thus the reconnection is FAST!

No η-dependence!

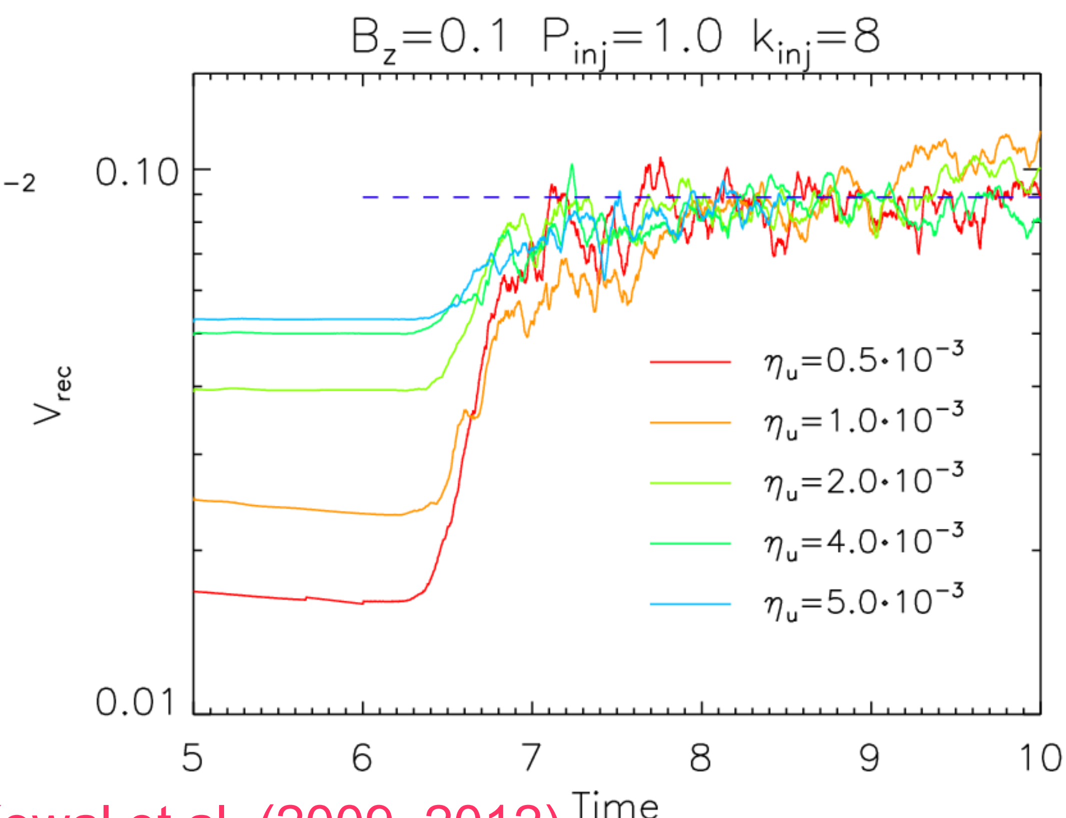

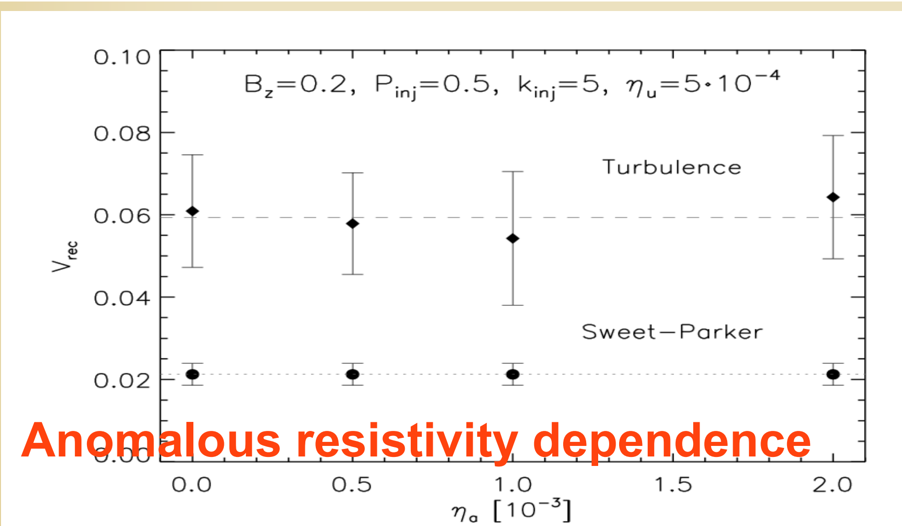

Anomalous resistivity dependence

Kowal et al. (2009, 2012)

Can reconnection generate turbulence?

A. Beresnyak (2013, arXiv:1301.7424)

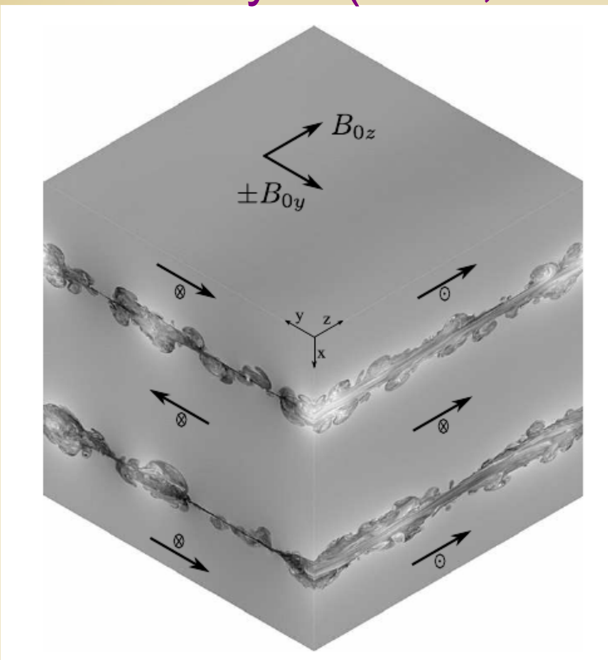

Fully periodic box up to 1536^3

Time evolution of the current layer width Δ

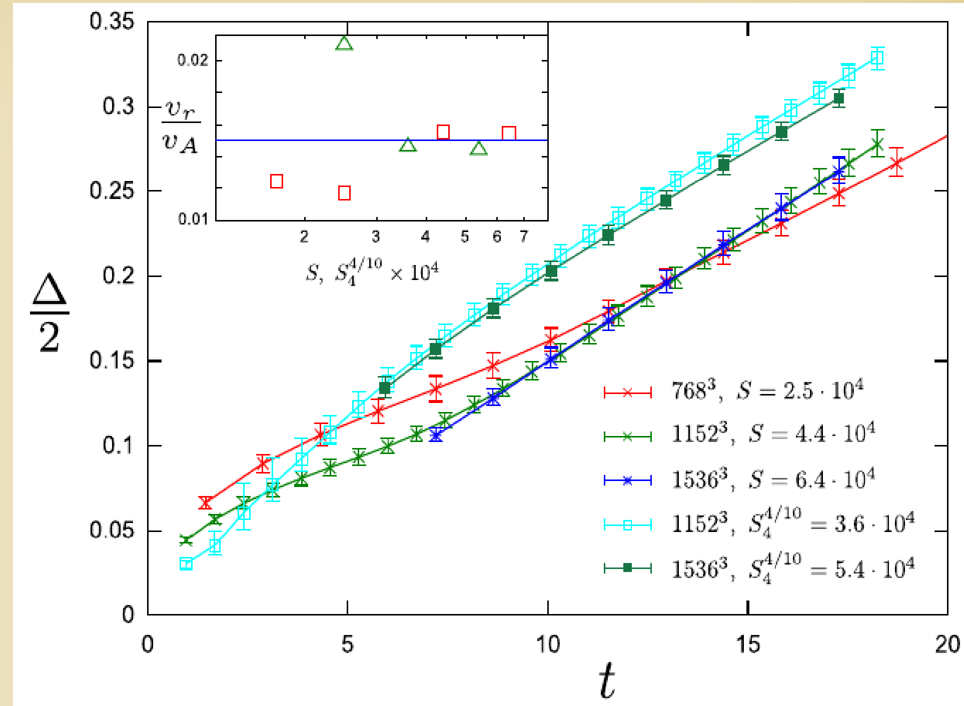

Oishi et al. (2015)

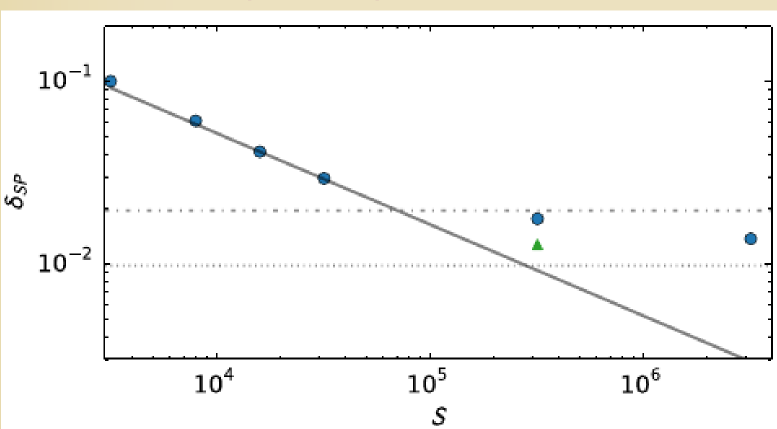

Huang & Bhattacharjee (2016)

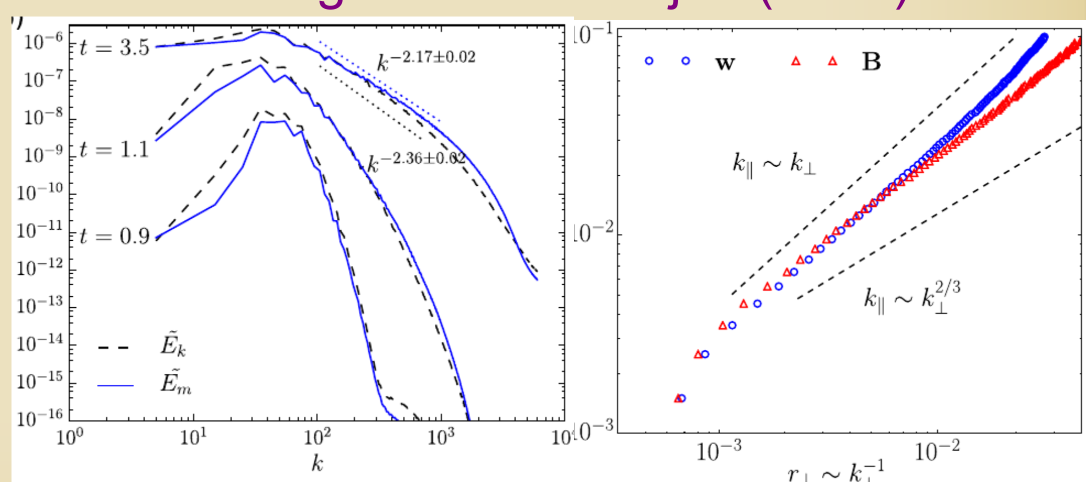

3D MHD processes alone produce fast (resistivity independent) reconnection without recourse to kinetic effects or external turbulence.

The resulting turbulence is **not** of the Goldreich-Sridhar (1995) type.

Can reconnection generate turbulence?

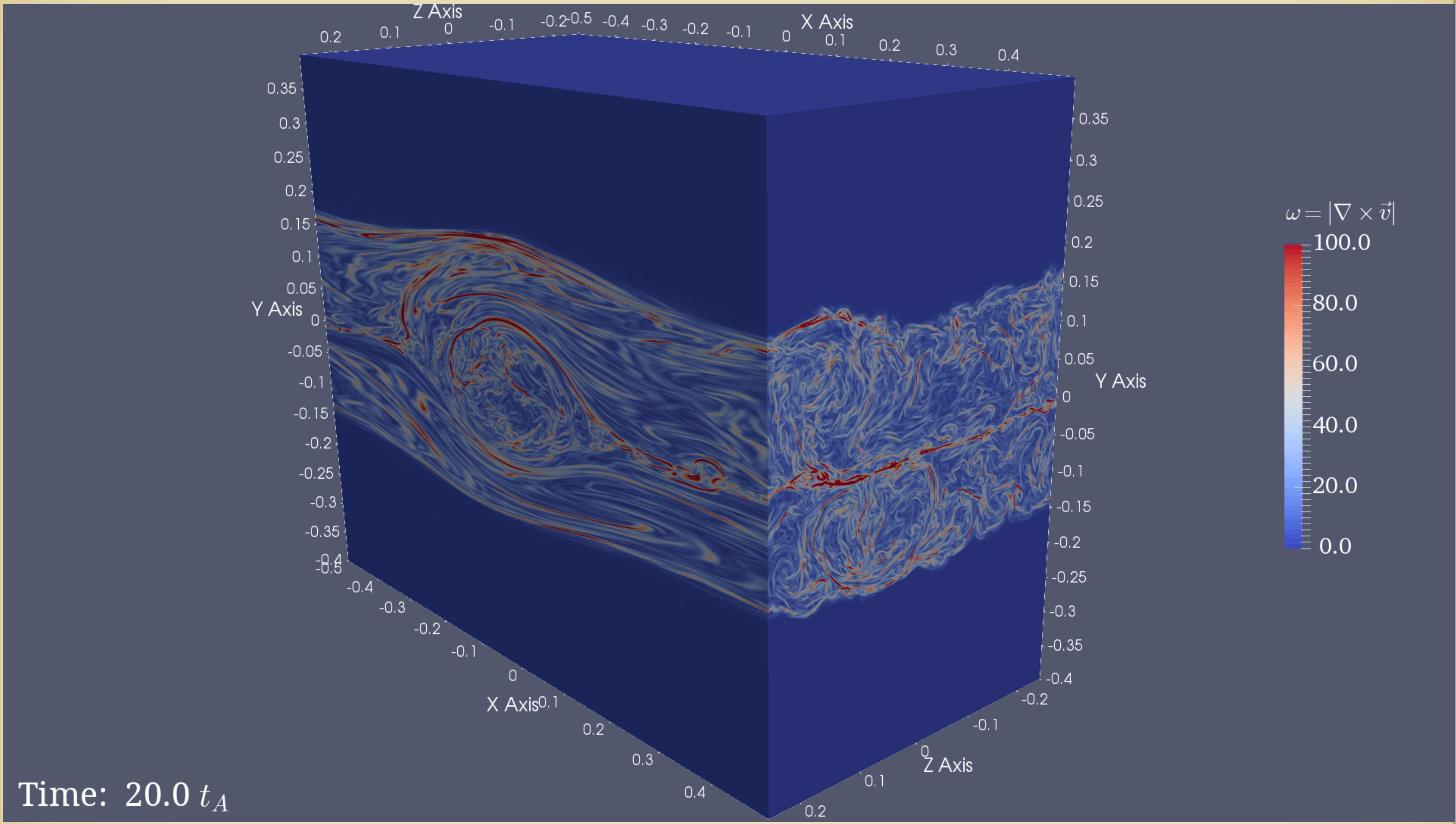

What are the properties of reconnection-driven turbulence?

Kowal et al. (2017)

Turbulent Region Thickness

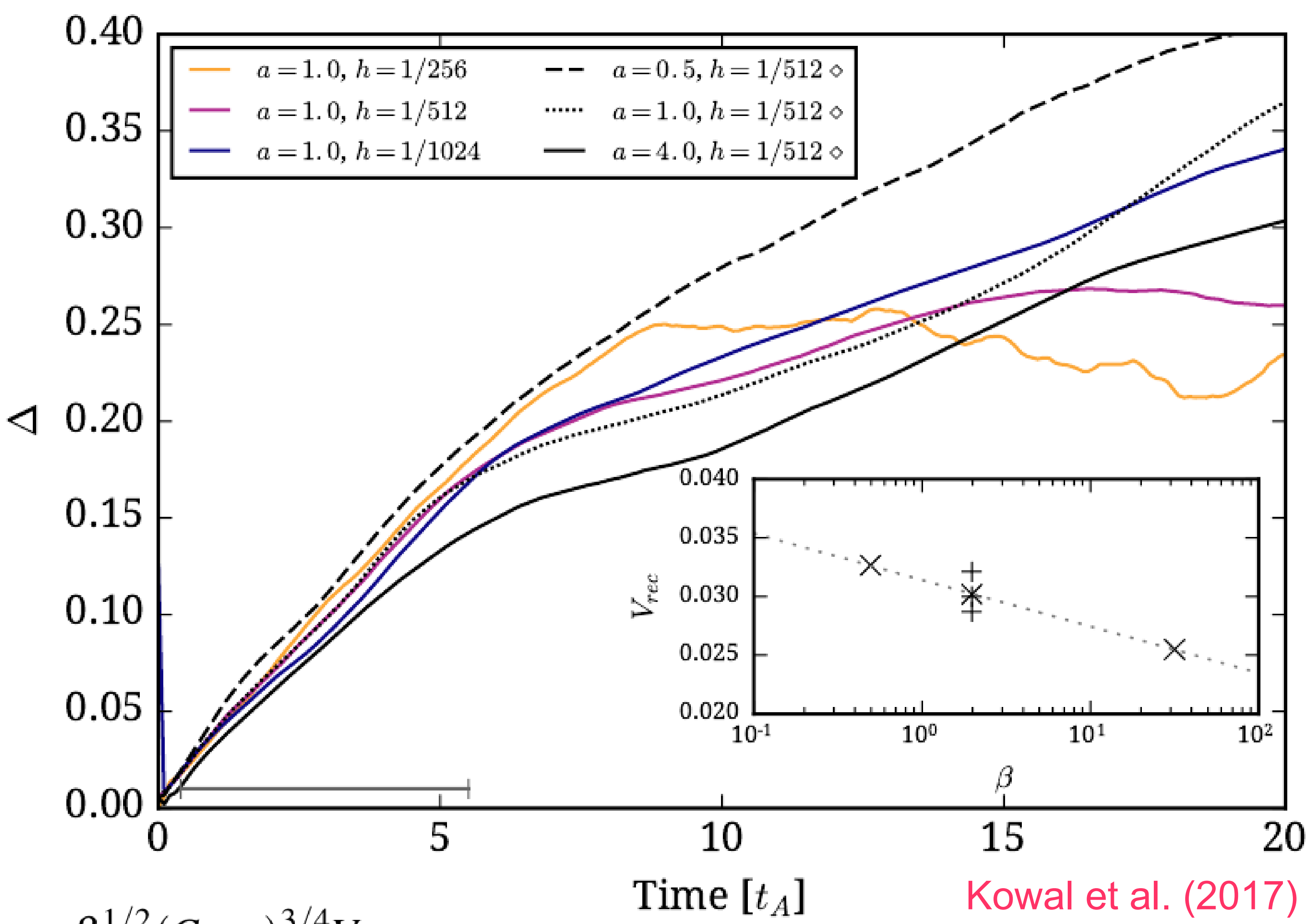

$$\frac{d\Delta}{dt} \approx g\beta^{1/2}(C_K r_A)^{3/4} V_{Ay}$$

Lazarian et al. (2014)

Continuous growth of the turbulent region. The growth rate depends on the plasma β and resolution.

Turbulence Properties – Power Spectra

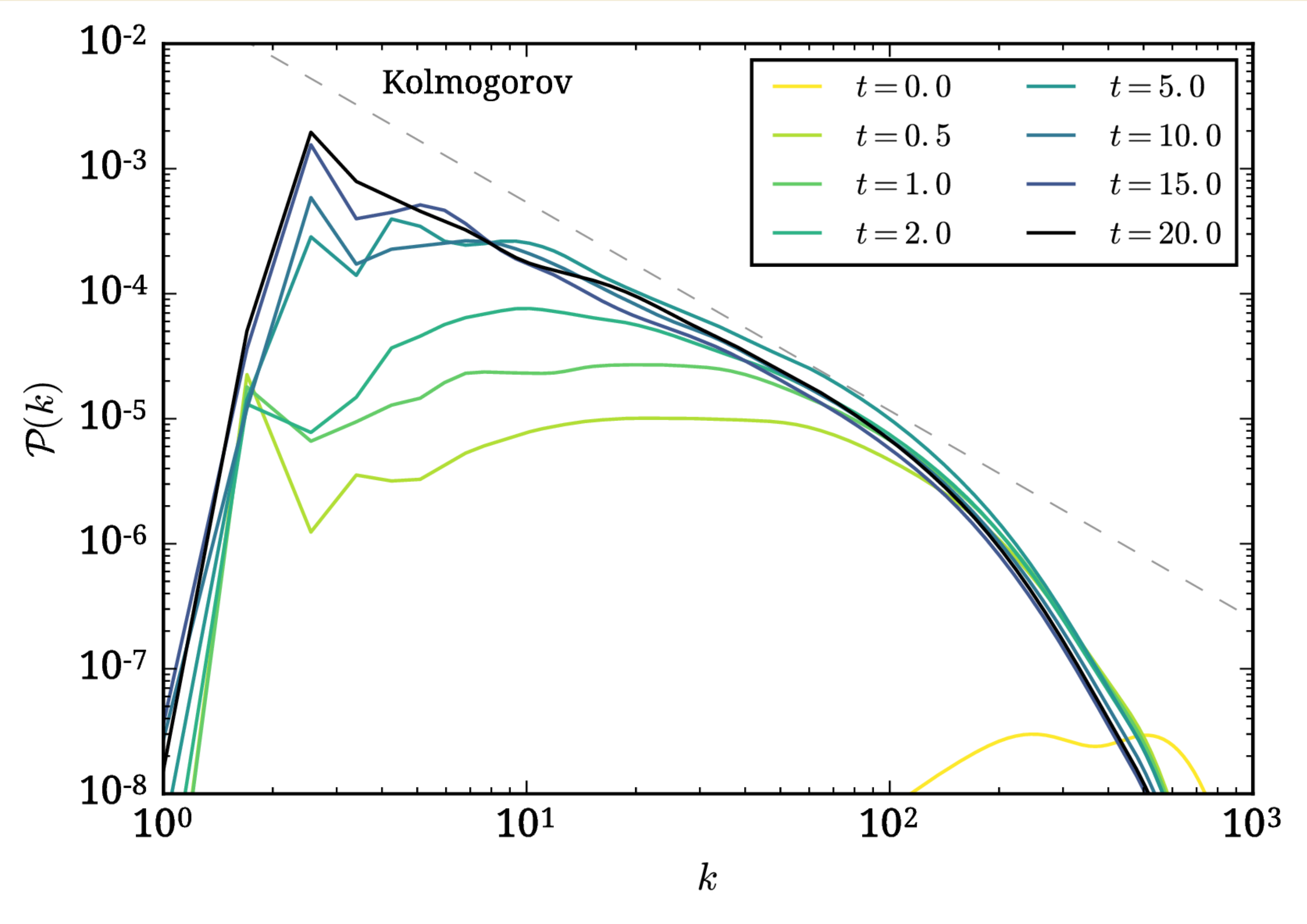

Velocity power spectrum in agreement with Kolmogorov and GS95 $\sim k^{-5/3}$.

Kowal et al. (2017)

Turbulence Properties – Anisotropy Scalings

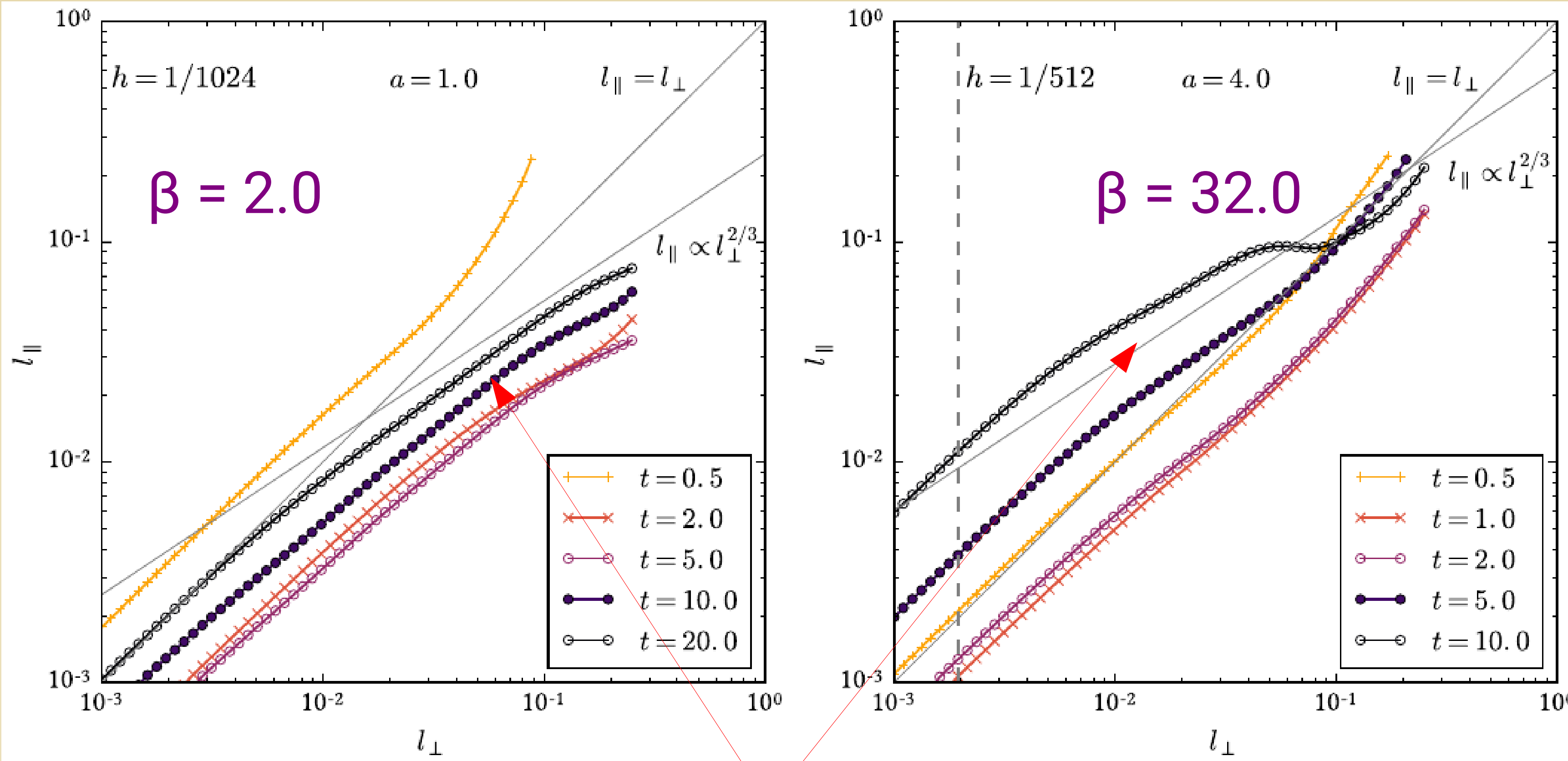

Anisotropy scaling of velocity fluctuations evolves to a scaling <u>compatible</u> with GS95 for scales not affected directly by the reconnection events.

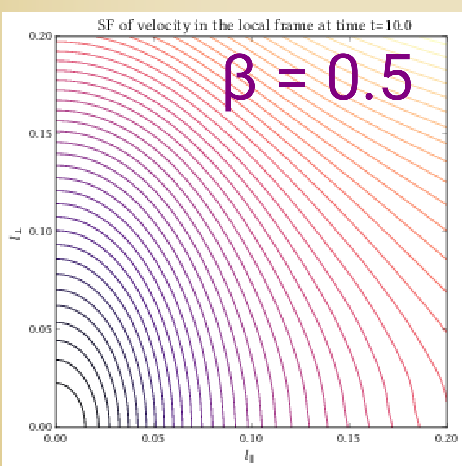

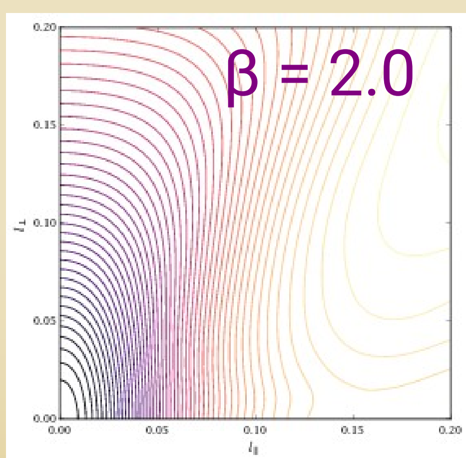

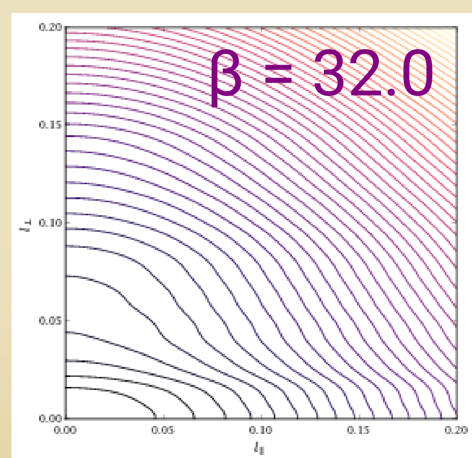

Kowal et al. (2017)

The change of velocity anisotropy with plasma β.

Driving Mechanism Candidate: Tearing Instability

Tearing Mode – a finite resistivity instability of a sheet pinch

(Furth & Killeen, 1963)

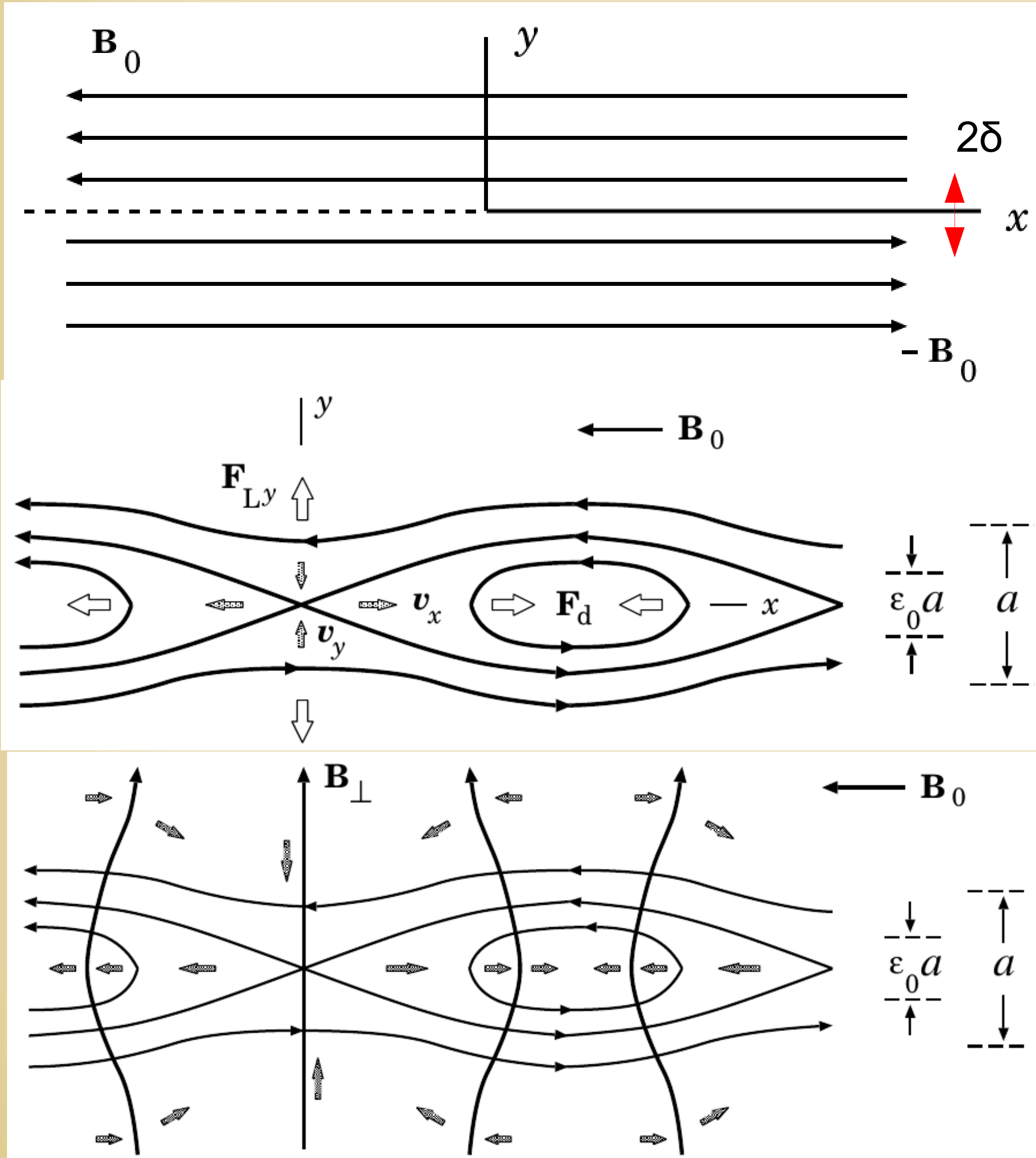

Instability condition:

$$k\delta \ll 1$$

Growth rate:

$$\omega\tau_A = \left(\frac{2}{\pi}\right)^{2/5} (k\delta)^{-2/5} S_\delta^{-3/5}$$

$$S_\delta = \frac{v_A \delta}{\eta}$$

The stabilizing effect of
transversal field:

$$(\omega\tau_A)^5 = \left(\tfrac{2}{\pi}\right)^2 (k\delta)^{-2} S_\delta^{-3} - \xi^2 S_\delta (\omega\tau_A)^4$$

$$\xi = B_n / B$$

Verneta & Somov (1987)
Somov & Verneta (1996)

Tearing Instability Analysis – Thickness Distribution

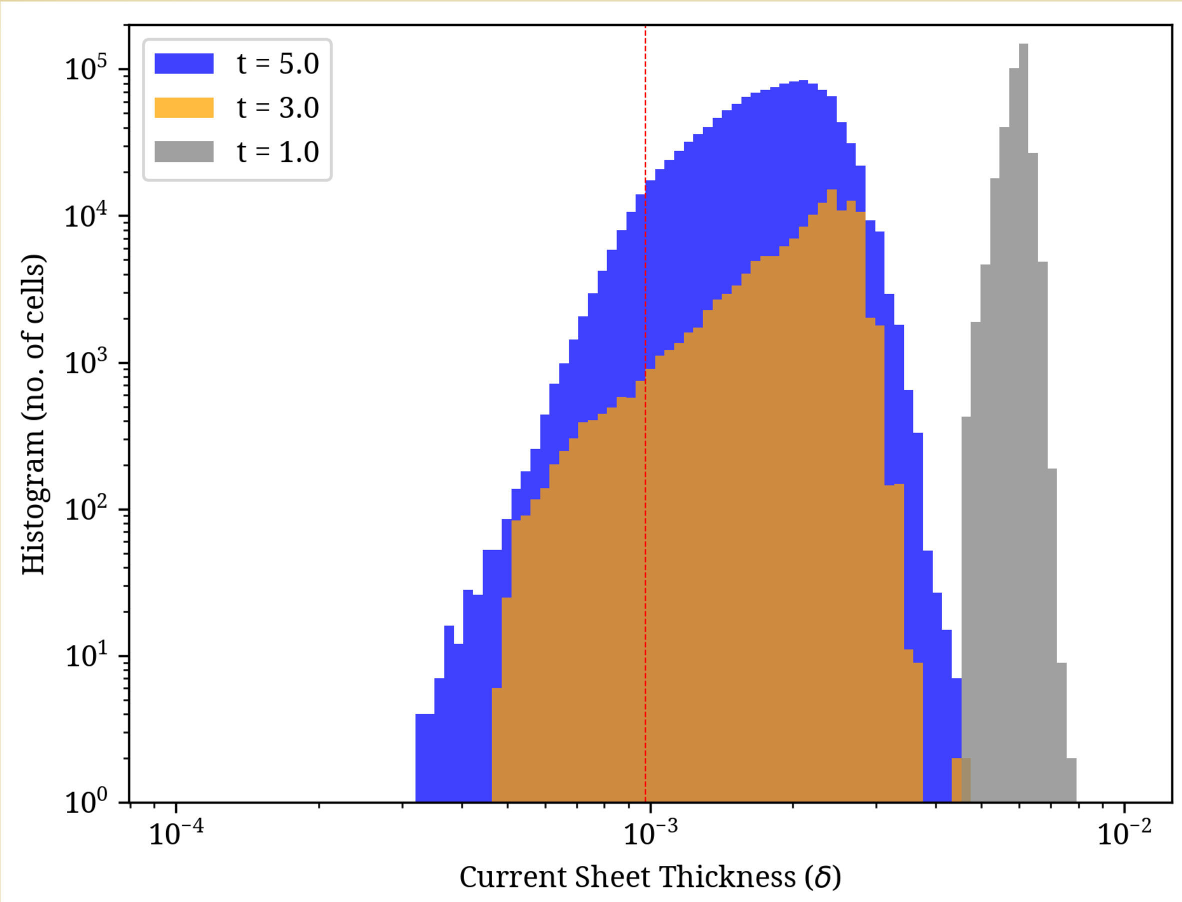

Kowal et al. (2017, in prep.)

Prandtl number Pr = ν/η = 1, explicit dissipation ν = η = 10^{-5}

Plasma β = 0.5

Box size: 1.0 x 4.0 x 1.0

Effective resolution (AMR): 1024×4096×1024

Tearing Instability Results – Stability Region

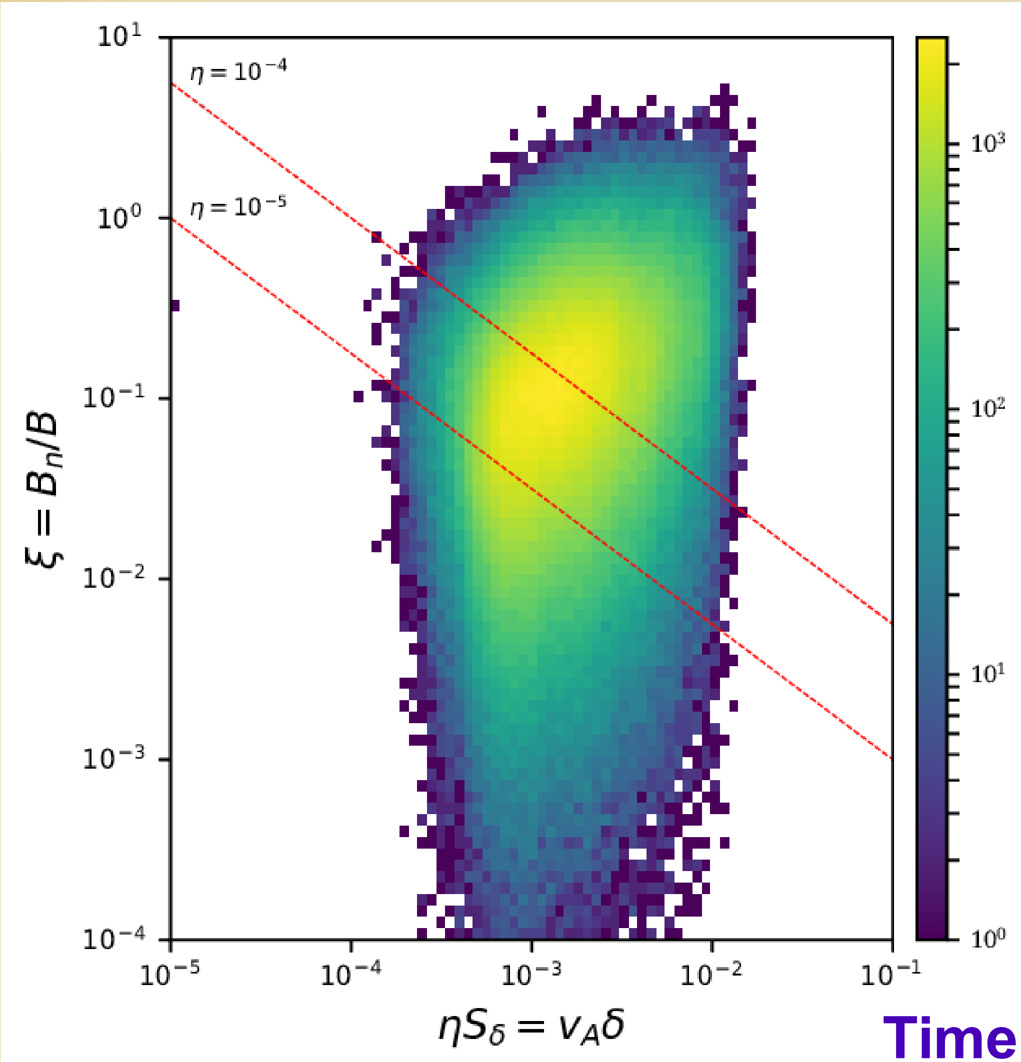

Time = 5.0 t_A

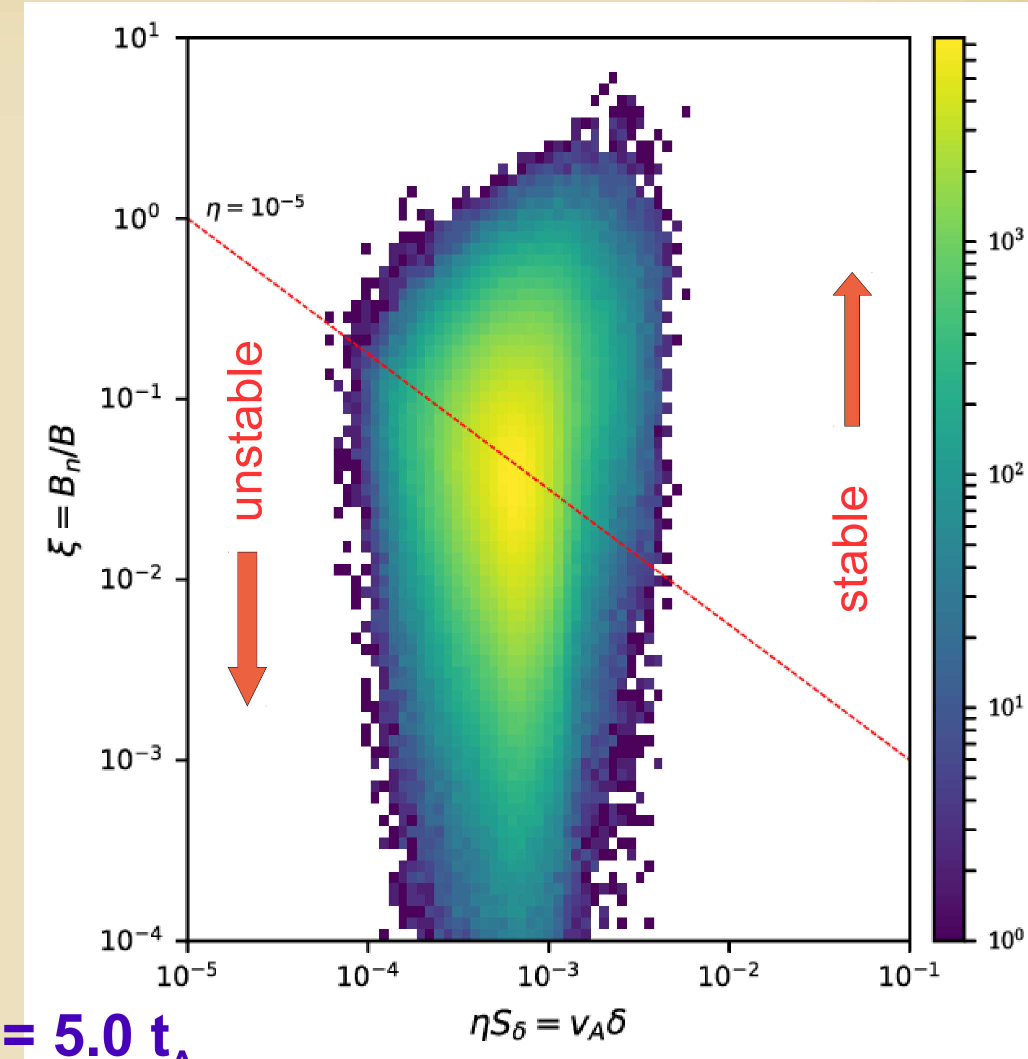

Prandtl number Pr = ν/η ≈ 1,
numerical dissipation

Prandtl number Pr = ν/η = 1,
explicit dissipation ν = η = 10^{-5}

Kowal et al. (2017, in prep.)

Tearing Instability Analysis – Growth Rate

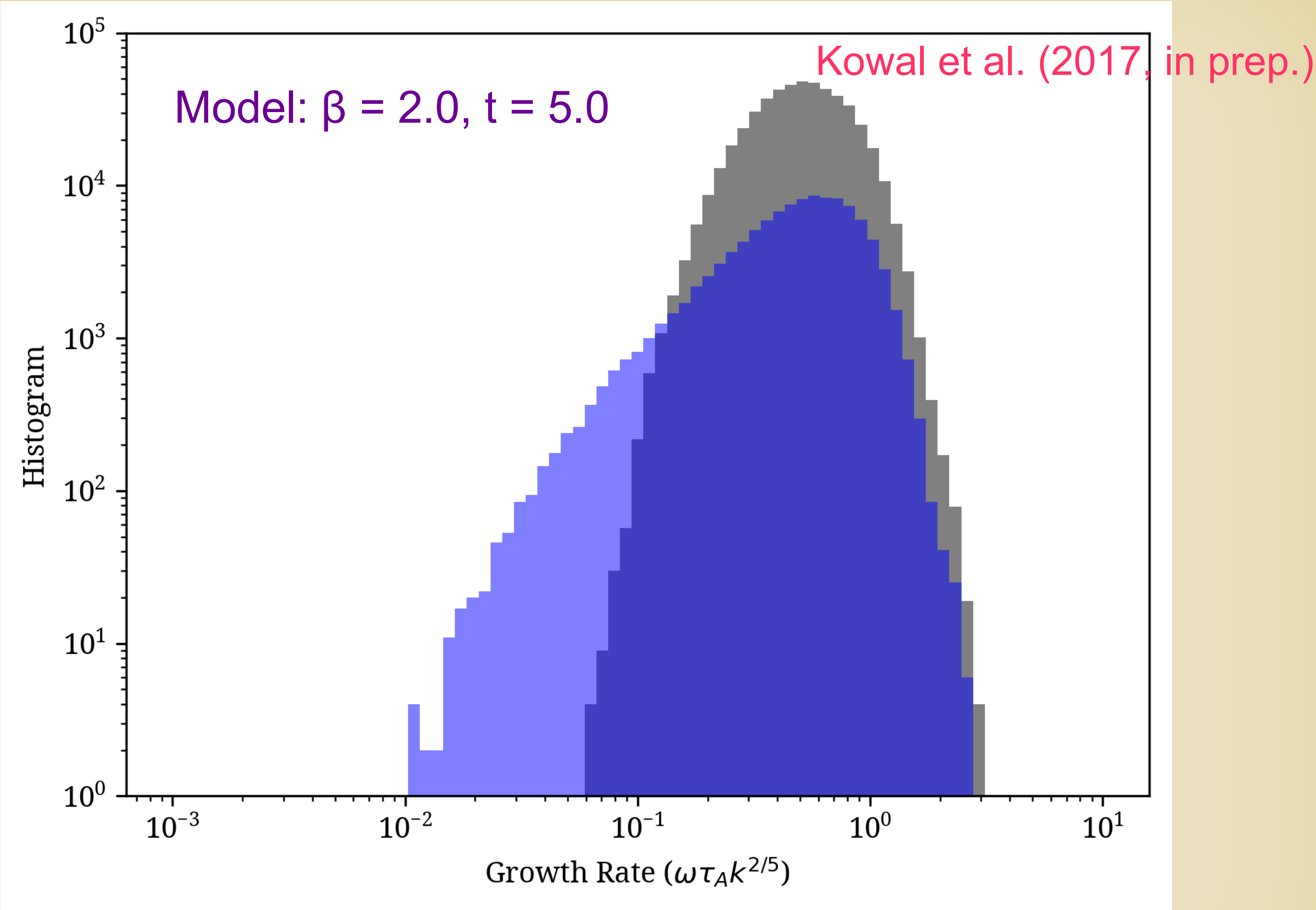

Growth rate:

$$(\omega\tau_A)^5 = \left(\frac{2}{\pi}\right)^2 (k\delta)^{-2}\, S_\delta^{-3} - \xi^2 S_\delta\,(\omega\tau_A)^4$$

Driving Mechanism Candidate: Kelvin-Helmholtz Instability

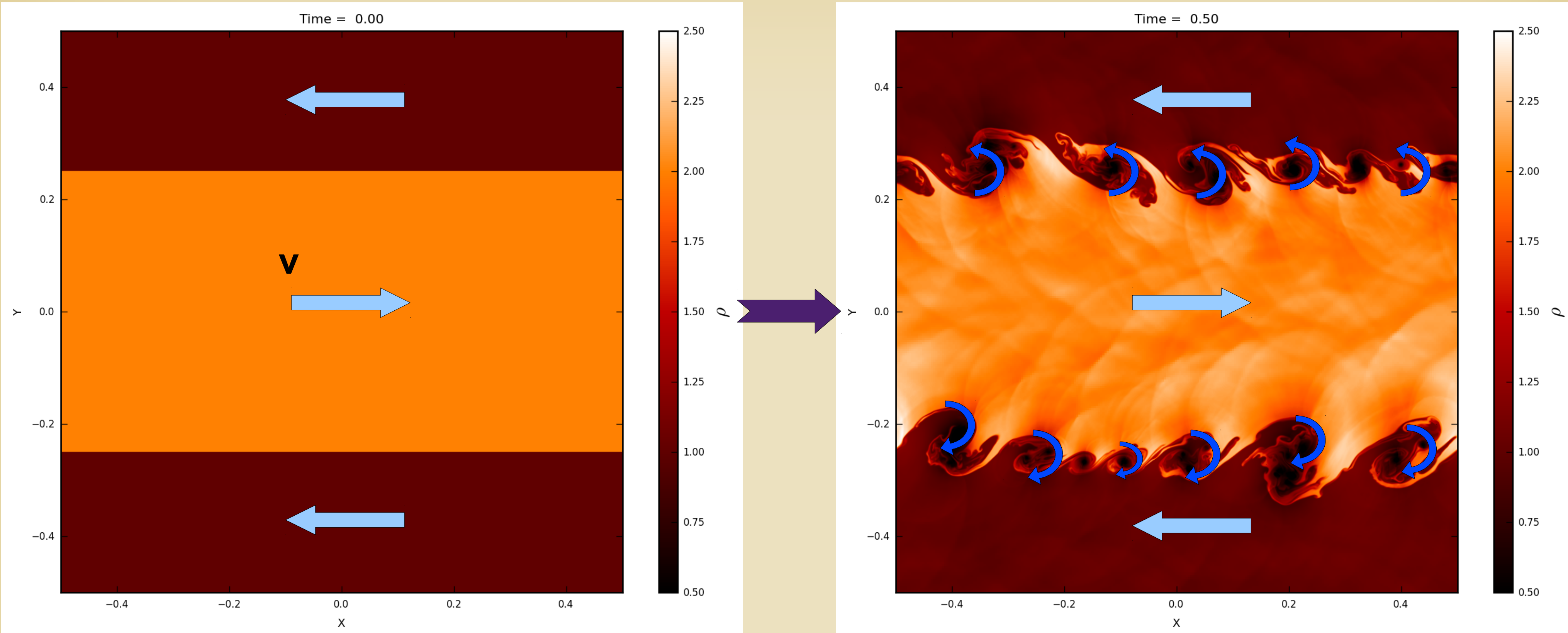

<u>Incompressible case</u> (Chandrasekhar, 1961)

$$\omega\tau_A = 2\pi k\sqrt{\frac{1}{2}\left(\frac{\Delta U}{v_A}\right)^2 - 1}$$

<u>Compressible case</u> (Miura & Pritchett, 1982)

$$\left(\mathcal{M}_A^2 + \mathcal{M}_s^2 - \frac{4\left(\vec{k}\cdot\vec{B}_0\right)^2}{k^2}\right) > \frac{1}{4}\mathcal{M}_s^2\mathcal{M}_A^2$$

$$\mathcal{M}_s = \frac{\Delta U}{c_s} < 2 \quad \text{and} \quad \mathcal{M}_A = \frac{\Delta U}{v_A} > 2 \quad \text{for} \quad \vec{k} \parallel \vec{B}$$

Kelvin-Helmholtz Instability Results

Kowal et al. (2017, in prep.)

β = 0.5

β = 32.0

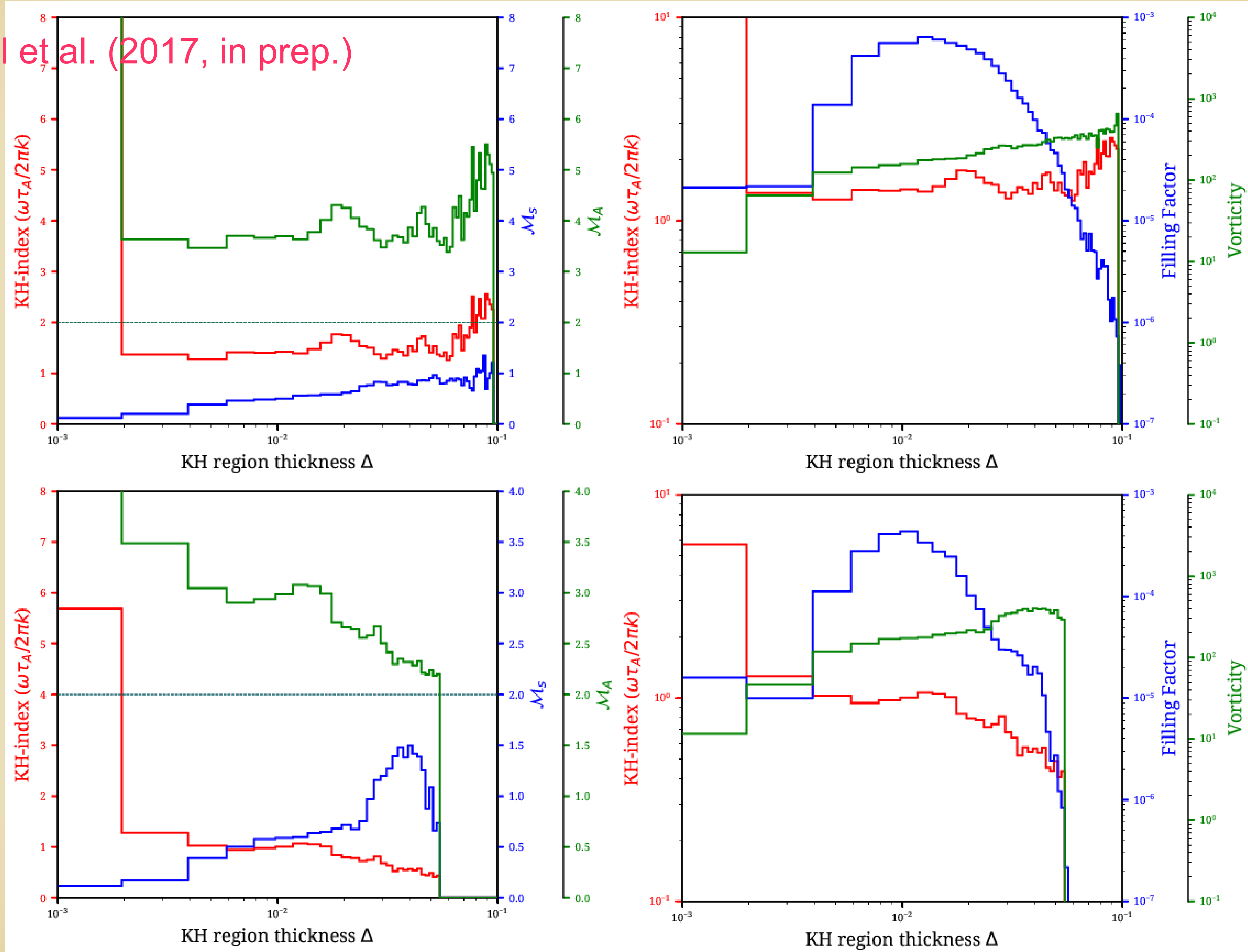

Conclusions

- Models with different types of isotropic turbulence driving (in Fourier and real space, driving of velocity and magnetic field, Kowal et al. 2012) show results compatible with the original testing of Lazarian-Vishniac model (Kowal et al. 2009), where V_{rec} is significantly enhanced and grows as $\sim V_T^2$ and $\sim (l_{inj}/\Delta)^{3/4}$, and in 3D is independent of the resistivity.

- In the presence of initial noise, reconnection can generate turbulence, effectively accelerating itself, potentially resulting in self-sustained fast reconnection.

- The generated turbulence approximates the GS95 model at larger scales once a broad turbulent region is developed (at later times). Smaller scales are strongly affected by the ejection flows from the local reconnection events.

- Two instabilities, namely tearing mode and Kelvin-Helmholtz instability, were analyzed as candidates for the turbulent driving mechanisms. Both processes are present in the numerical models and show comparable growth rates. However, the tearing mode might be significantly suppressed by the transversal field produces by turbulence.